

3-26-2003

The first 80-hour continuous lidar campaign for simultaneous observation of mesopause region temperature and wind

C. Y. She

J. Sherman

Titus Yuan
Utah State University

B. P. Williams

K. Arnold

T. D. Kawahara

See next page for additional authors

Follow this and additional works at: http://digitalcommons.usu.edu/physics_facpub

 Part of the [Physics Commons](#)

Recommended Citation

She, C. Y., J. Sherman, T. Yuan, B. P. Williams, K. Arnold, T. D. Kawahara, T. Li, L. F. Xu, J. D. Vance, P. Acott and D. A. Krueger (2003), The first 80-hour continuous lidar campaign for simultaneous observation of mesopause region temperature and wind, *Geophys. Res. Lett.* 30, 10.1029/2002GL016412.

This Article is brought to you for free and open access by the Physics at DigitalCommons@USU. It has been accepted for inclusion in All Physics Faculty Publications by an authorized administrator of DigitalCommons@USU. For more information, please contact dylan.burns@usu.edu.



Authors

C. Y. She, J. Sherman, Titus Yuan, B. P. Williams, K. Arnold, T. D. Kawahara, T. Li, L. F. Xu, J. D. Vance, P. Acott, and D. A. Krueger

The first 80-hour continuous lidar campaign for simultaneous observation of mesopause region temperature and wind

C. Y. She, Jim Sherman,¹ Tao Yuan, B. P. Williams, Kam Arnold, T. D. Kawahara,² Tao Li, Li Fang Xu, J. D. Vance, P. Acott, and David A. Krueger

Department of Physics, Colorado State University, Fort Collins, Colorado, USA

Received 8 October 2002; revised 18 December 2002; accepted 24 December 2002; published 26 March 2003.

[1] The Colorado State Sodium lidar has been upgraded to a two-beam system capable of simultaneous measurement of mesopause region temperature and winds, day and night, weather permitting. This paper reports the initial result of the first campaign, conducted in April 2002, with a total of 145 hours of observation including an 80-hour continuous data acquisition of temperature and zonal wind. The contour plots of the continuous data set show considerable coherence and activities of upward propagating waves, with a maximum day-night difference of 15.5 m/s in zonal wind at 88 km and of 10 K in temperature at 92 km. Oscillations at periods of 10-hour in temperature and 16-hour in zonal wind, implicating nonlinear interactions, can be identified. Decomposition of the time series into tidal periods, resulted in very good agreement with the GSWM00 predictions of diurnal tide. The observed altitude dependence in diurnal amplitudes and phases is consistent with the presence of a significant upward propagating wave, accompanying and modulating the main diurnal tide. *INDEX TERMS:* 3332 Meteorology and Atmospheric Dynamics: Mesospheric dynamics; 3384 Waves and tides. *Citation:* She, C. Y., J. Sherman, T. Yuan, B. P. Williams, K. Arnold, T. D. Kawahara, T. Li, L. F. Xu, J. D. Vance, P. Acott, and D. A. Krueger, The first 80-hour continuous lidar campaign for simultaneous observation of mesopause region temperature and wind, *Geophys. Res. Lett.*, 30(6), 1319, doi:10.1029/2002GL016412, 2003.

1. Introduction

[2] Over the past fifteen years or so, observations of the mesopause region by metal resonance lidars, capable of high temporal and vertical resolution, have contributed considerably to our understanding of climatology and dynamics in this important region of the atmosphere. Most of these observations were limited to nocturnal temperatures [von Zahn *et al.*, 1996; She *et al.*, 2000]. Since global temperature and wind fields are coherently coupled, and observations under sunlit conditions are as important, the capability for simultaneous lidar observation of temperature and wind over complete diurnal cycles is of obvious interest, especially for studies of dynamics. Initial results of daytime wind measurements were published [Yu

et al., 1997; States and Gardner, 1998]. A recent study comparing collocated lidar and radar wind measurements [Franke *et al.*, 2001], however, reported nighttime agreement along with a huge daytime discrepancy between the two instruments.

[3] Since a Faraday filter can reject sky background by a factor of 6000–8000, it can be used as an effective frequency discriminator against sky background. Its success depends, to a great extent, on its stability during data acquisition. This requirement is much more stringent for wind measurements. For this reason, the success in using Faraday filters for daytime simultaneous temperature and wind measurements comes several years after the report of daytime temperature measurements [Chen *et al.*, 2000].

[4] The purpose of this paper is to report the result of our initial observation of mesopause region temperature and zonal wind over complete diurnal cycles. The key data set was acquired between 2.3UT, April 22nd and 11.7UT, April 25th, a continuous 80 hours of simultaneous measurement of temperature and zonal wind. We perform the standard analysis to illustrate the richness of dynamical information (tide, wave and interaction) that may be extracted from this first data set. Though various radar techniques have been used widely over the years to characterize tidal perturbations in wind, the work reported here marks the beginning of a new observation technique that is capable of interrogating both temperature and wind perturbations in high spatial resolution, simultaneously and continuously.

2. Colorado State Two-Beam Narrowband Na Lidar

[5] In response to the need of TIMED science objectives, the Colorado State narrowband Na lidar began its upgrade from a one-beam to a two-beam system in 1999, designed for the simultaneous measurement of mesopause region Na density, temperature, zonal and meridional wind profiles with both daytime and nighttime capability. The measurement precision of our lidar system for temperature and wind with 2 km spatial resolution and 1 hr integration were estimated for each beam under nighttime fair sky conditions to be, respectively, 0.5 K and 1.5 m/s at the Na peak (92 km), and 5 K and 15 m/s at the edges (81 and 107 km) of the Na layer. Depending on the purpose of the analysis, the temporal resolution may be made between 10 min and several hours.

[6] To permit observation under sunlit condition, a pair of in-house constructed Faraday filters were used. With the received signal being reduced by a factor of 4–5, the measurement uncertainty is larger by a factor of ~2.5 when

¹Now at Department of Physics, Indiana University of Pennsylvania, Indiana, PA, USA.

²Permanently at Faculty of Engineering, Shinshu University, Nagano, Japan.

the Faraday filter is in use. It took us quite sometime to achieve the stringent requirement on the stability (against thermal fluctuations) of the Faraday filter for wind measurements and to improve the device that corrects an instrumental line-of-sight wind bias of 2–10 m/s in real time. Though still by no means a turn-key instrument, the Colorado State two-beam narrowband Na lidar is fully functional by the year 2002, producing the expected data quality.

3. Initial Data Set of April 2002

[7] The first campaign was conducted between April 8th (day 098) and April 30th (day 120), 2002, yielding a total of 145 hours (with 59.5 hours under sunlit condition) of observation. Significantly, we were blessed by fair Colorado weather and made a continuous 81-hour observation (from day 112 to day 115) with only one hour data gap. In this campaign, one beam was pointed at Zenith and the other to the East, 30° from Zenith. The data collected from the tilted, East beam are integrated hourly and processed at 2 km (4 km) vertical resolution for nighttime (daytime) data. The data from the Zenith beam are mainly used to assess the performance of the Faraday filters and the wind-bias correction instrument, though they have also been analyzed to produce independently measured temperature profiles. In this paper, we present the initial science results from this first set of 80-hour continuous observation with both temperature and zonal wind information, covering much of the mesopause region (82–98 km), supplemented by additional data acquired in the month of April. For quantitative analysis, we form two data sets. Data set I, labeled as (112-5), uses data from the 80-hour continuous observation only; data set II, labeled as (April), includes all data in April.

4. Dynamics Revealed by the Continuous 80-Hour Observation

[8] The salient features in a continuous data set resulting from multi-day, spatially resolved observation, with complementary field variables measured, lie in its ability to discern spatial and temporal development of waves and tides during the period. Contours of temperature and zonal wind in time-altitude were plotted for data set I, as shown in Figure 1. The x-axis reference is the local midnight, i.e., 0 h, LST (local solar time) or 7 h, UT of day 112. Even with the use of Faraday filters, the signal-to-noise under sunlit conditions is not as good, limiting the altitude range for the daytime observation to between 82 and 98 km as can be seen in Figure 1. An obvious and common feature in these temperature (Figure 1a) and zonal wind (Figure 1b) contours is the presence of correlated 12- and 24-hour oscillations of downward propagating phases with the 12-hour oscillation having longer vertical wavelength. The 12-hour oscillation is clearly more pronounced above 93 km, while the 24-hour component appears to be stronger below 93 km.

[9] To gain a general appreciation of the diurnal variation in this data set, we perform 4 different averages, denoted by $\text{avg}[19-100]$, $\text{avg}[18-6]$, $\text{avg}[6-18]$, and ‘const’, representing, respectively, averages of all the data, night (18–6 h, LST), day (6–18 h, LST), and the constant term from the

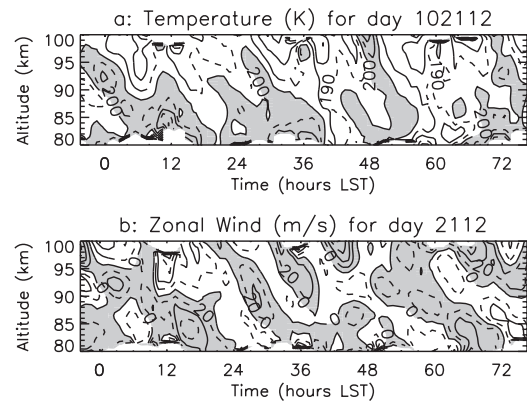


Figure 1. Contours of (a) temperature, with 20 K interval and values above 200 K gray-shaded, and (b) zonal wind, with 20 m/s interval and positive values gray-shaded, of an 80-hour observation (local midnight of day 112 is $x = 0$).

tidal fit (see below). Here, we divide data equally into night and day according to LST. These averages using data set I from the east beam are plotted in Figures 2a and 2b. The small difference seen between profiles $\text{avg}[19-100]$ and ‘const’ is the result of one hour data gap still existed along with the statistical weighting used in the tidal analysis to determine the ‘const’ term. A maximum day-night difference, 10 K at 92 km in temperature and 15.5 m/s at 88 km in zonal wind, is observed, implicating that tidal and other wave activities are significant and that a continuous data set facilitates their observation. Though the mean zonal wind of ~ 10 m/s at the end of April is consistent with TIMED-GCM [Roble, 2000] climatology prediction, day-to-day variability is expected. In Figure 2a, we also plotted our 8-year nocturnal temperature climatological mean between days 112 and 115 and the nighttime mean of April 2002 (data set II). One notices considerable difference (7 K at 92 km and 5.5 K at 84 km) exists between nighttime mean of data set I and the climatological mean. This difference is much reduced (to 4 K at 92 km and 0 K at 84 km), when data set II covering the month of April is used.

[10] To facilitate the detection of various wave features, Lomb spectral densities were calculated using data set I and plotted in Figures 3a and 3b, respectively for temperature and zonal wind. In addition to the expected 24- and 12-hour periods and a few minor features, we see a clear 16-hour component between 82 and 94 km in the zonal wind, and a 10-hour component between 86 and 93 km in the temperature. One could attribute these features to nonlinear interactions, between semi-diurnal tide and quasi 2-day planetary wave [Palo *et al.*, 1999], resulting in difference and sum frequency excitation, nominally designated as 16- and 9.6-hour oscillations since their first observation [Manson and Meek, 1990]. That the 12-hour oscillation is conspicuously absent, or at least very weak at altitudes where the 10-hour and 16-hour signal are strong is interesting but not problematic because the interaction does not have to be local [Walterscheid and Vincent, 1996]. These waves are likely generated below 80 km where 2-day waves, though intermittent, are stronger; as they propagate up, they could be trapped in the region below 93 km where it could grow at the expense of the 12-hour oscillation. The

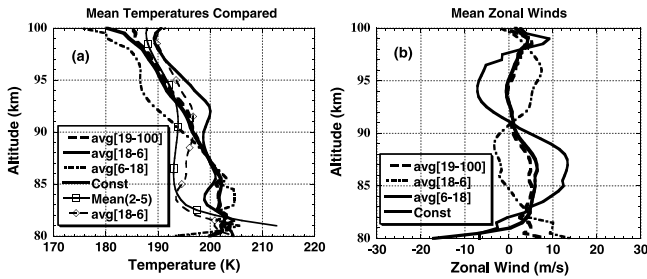


Figure 2. Mean, night (18-6), day (6-18) and ‘const’ of data set I are in bold dashed, dashed-dot, solid and bold solid for (a) temperature and (b) wind. Also in (a) are nocturnal climatology in thin solid with squares, and that of April in thin dashed with diamonds.

16-hour oscillation could also be a sum secondary wave due to diurnal tide and quasi-two-day wave, as significant Lomb power are seen for all 3 components in Figure 3a. More generally, cases of interaction with planetary waves in the mesopause region are being studied in observations [Pancheva *et al.*, 2002] and in realistic simulation [Hagan and Roble, 2001]. The observation of these secondary oscillations in both temperature and wind for the first time has demonstrated the value of a continuous multiple day data set in revealing coherence in wave dynamics and the scientific potential enabled by the new lidar techniques.

5. Observed 24-hour and 12-hour Oscillations

[11] With a long data set, the time series of temperature, $T(z, t)$, and zonal wind, $u(z, t)$, at each altitude, can be decomposed into the sum of a constant (mean) and harmonic terms with periods of 24, 12, 8 and 6 hours. The analysis procedure of Colorado State lidar outputs a measurement uncertainty resulting from photon noise for each measured value, temperature or wind. In addition to the measurement uncertainty, there is unavoidable geophysical variability (noise) due to perturbations not included in the analysis model, in this case, fluctuations other than the constant (mean) and 4 tidal components. We estimated geophysical variability from the minimum standard deviation of the hour-averaged measured values at an altitude near the peak of the Na layer in the 2-hour duration centered at the midnight. Our reasoning is that if the 4 oscillations with tidal periods were the only perturbations from the mean value, the measured values at different mid-nights

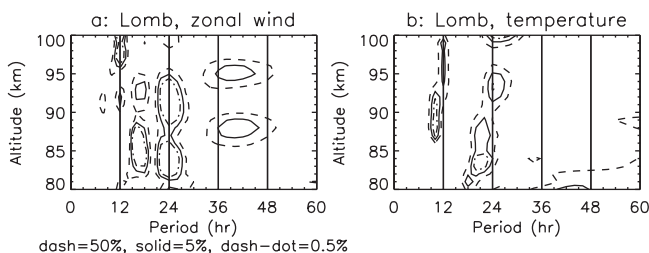


Figure 3. Lomb power contour altitude (y in km)-period (x in hour) plots of (a) zonal wind and (b) temperature. Dashed, solid, and dashed-dot contours represent 50%, 5%, and 0.5% probability that the Lomb power may be due to random noise.

near the Na peak, where the measurement uncertainty is negligible, should be the same. Thus, the minimum variability so determined, 7.2 K and 16.4 m/s, respectively, for temperature and zonal wind, may be taken as the geophysical variability for the analysis. The least-squares fit is then performed by weighting the experimental data with the inverse of the sum of measurement and geophysical variances (square of standard deviation).

[12] We perform two separate tidal analyses. With analysis I and II using data set I and II, respectively. Since other than 8 to 9 daytime hours each in day 103 and 108, most of the daytime data are contained in the 80-hour continuous observation, we expect the resulting 24-hour oscillation to be similar between the two analyses.

[13] The diurnal amplitude and phase of zonal wind are shown in 4(a) and 4(b), respectively. On the same graphs, we also plotted the April and May simulation of GSWM00 (Global Scale Wave Model) [Hagan *et al.*, 1999] for comparison. There is very good agreement in diurnal phase between observation and prediction in zonal wind. The agreement in diurnal amplitude is also good between 86 km and 94 km. However, while the GSWM00 amplitude continues to increase to 30 m/s at 100 km, the observed amplitude increases to a maximum of 32 m/s at 84 km and decreases to a minimum of 6 m/s and 13 m/s for (112-5) and (April), respectively. To the first order, the altitude dependence of diurnal amplitude can be understood in terms of the interference between two waves. We could take the agreement between model and observation in diurnal phase of (112-5) between 86 km and 90 km to depict the main tidal mode with an estimated vertical wavelength of ~ 12.5 km. The slope of the diurnal phases between 82 and 86 km, and between 91 and 95 km, Figure 4b, are similar, suggesting the existence of another upward propagating mode with vertical wavelength of ~ 41.5 km. The spatial interference between this second mode and the main tidal

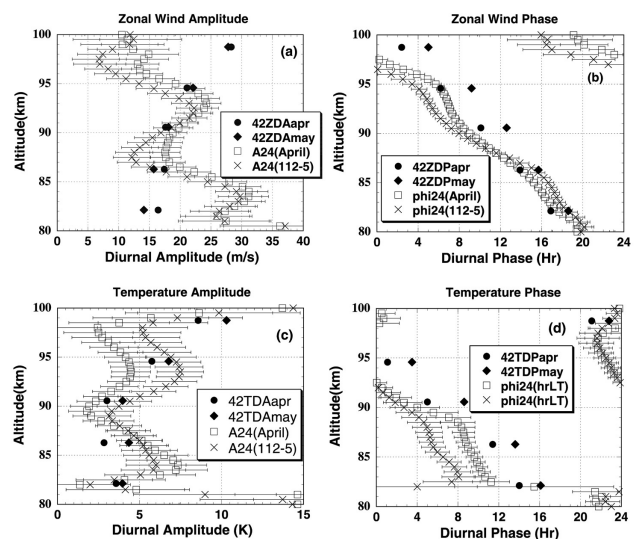


Figure 4. Diurnal tide amplitudes and phases, respectively (a) and (b) for zonal wind, and (c) and (d) for temperature. Solid circles and solid diamonds are GSWM00 April and May output; open squares and crosses are, respectively April and (112-5) data.

mode produces a beat pattern with a calculated separation between the maxima or minima of ~ 9.5 km, consistent with those observed in the diurnal amplitude profile.

[14] There exists also a wavy pattern in the temperature diurnal amplitude profile, Figure 4c. In the same manner, we could identify two propagating waves from the slope of temperature of diurnal phase, Figure 4d, with vertical wavelengths of ~ 15 km (designated tidal mode) and 27 km (the second mode). Interestingly, the interference of these two modes gives again a beat with the separation between the maxima or minima ~ 9.5 km consistent with the observed temperature diurnal amplitude. Since similar modulation in the temperature diurnal amplitude profile was also observed in springs, 1997 and 1998 [She et al., 2002], it may be a prevailing feature over Fort Collins. Continued observation in zonal wind is required to further substantiate this supposition. Though the nature of the observed second wave with longer vertical wavelength is not clear, the excitation of secondary waves resulting from the mean wind effect or from W1 tide/S1 planetary wave interaction was confirmed in model studies [Hagan and Roble, 2001]. Other than the observed beat pattern, which modulates the tidal amplitude, the agreement between the GSWM00 prediction and the observed 24-hr amplitude is good for both temperature and zonal wind.

[15] Though analyzed, we do not report the 12-, 8- and 6-hour oscillations here. Briefly, the semi-diurnal amplitudes for temperature and zonal wind amplitude are larger than GSWM00 prediction by 50% to 100%. Compared to the semi-diurnal oscillation, the 8- and 6-hour amplitude is between comparable to a factor 2 smaller in temperature, and a factor of 2 to 4 smaller in zonal wind.

6. Discussion and Conclusion

[16] A lidar campaign, measuring mesopause region temperatures and zonal wind in April 2002, including a 80-hour continuous data set, was completed. Comparing the averages between night (18-6, LST) and day (6-18, LST) of the 80-hour continuous data set, dynamical coherence resulting from tidal and other waves became evident. A significant difference between the night mean of this data set and the nocturnal climatology is noted; this difference however decreases when all data in April are included. The associated Lomb power plots revealed the presence of waves with 10-hour and 16-hour period, possibly resulting from nonlinear interactions between semidiurnal (or diurnal) tide and 2-day wave.

[17] A harmonic analysis including 24-, 12-, 8- and 6-hr periods was performed on both temperature and zonal wind profiles using the 80-hr continuous data set (Analysis I) and all 145 hours of data collected in April (Analysis II). The resulting amplitudes and phases of the 24-hour oscillation were compared to the prediction of GSWM00 migrating tidal model. In accord with the published studies [She et al., 2002; Pancheva et al., 2002], the 24-hr phases for both temperature and zonal wind are in very good agreement with the model prediction. The similarity between zonal wind and temperature diurnal amplitude profiles is intriguing, suggesting the presence of a second mode propagating along and modulating the migrating diurnal tide. The GSWM00 semidiurnal tidal amplitudes are 50% or a factor

of 2 smaller than observed (not shown) values. This discrepancy and the existence of second mode in the diurnal tide may both be related to the effect of planetary waves as hinted by the preliminary results presented here. Continued observation will reveal tidal variability at our site. Further model study incorporating planetary waves and collaborated observations with radar wind at different longitudes, being planned, will advance understanding at a deeper level.

[18] **Acknowledgments.** The lead author gratefully acknowledge the very helpful discussions with Maura Hagan, Richard Walterscheid, and Alan Manson. The work is supported by NSF grant ATM-00-03171 and NASA grant NAG5-10076.

References

- Chen, S. S., Z. L. Hu, M. A. White, D. A. Krueger, and C. Y. She, Lidar observations of seasonal variation of diurnal mean temperature in the mesopause region over Fort Collins, CO (41°N, 105°W), *J. Geophys. Res.*, *105*, 12,371–12,379, 2000.
- Franke, S. J., E. Stoll, R. J. States, and C. S. Gardner, Comparison of Na Doppler lidar and MF radar measurements of meridional winds in the mesosphere above Urbana, IL, *J. Atmos. Solar Terr. Phys.*, *63*, 1789–1796, 2001.
- Hagan, M. E., and R. G. Roble, Modeling diurnal tidal variability with the National Center for Atmospheric Research thermosphere-ionosphere-mesosphere-electrodynamics general circulation model, *J. Geophys. Res.*, *106*, 24,869–24,882, 2001.
- Hagan, M. E., R. G. Burrage, J. M. Forbes, J. Hackney, W. J. Randel, and X. Zhang, GSWM-98: Results for migrating solar tides, *J. Geophys. Res.*, *104*, 6813–6828, 1999.
- Manson, A. H., and C. E. Meek, Long-period (~ 8 –20 h) wind oscillations in the upper middle atmosphere at Saskatoon (52°N): Evidence for nonlinear tidal effects, *Planet. Space Sci.*, *38*, 1431–1441, 1990.
- Palo, S. E., R. G. Roble, and M. E. Hagan, Middle atmosphere effects of the quasi-two-day wave determined from a General Circulation Model, *Earth Planets Space*, *51*, 629–647, 1999.
- Pancheva, D., et al., Global-scale tidal structure in the mesosphere and lower thermosphere during PSMOS campaign of June–August 1999 and comparison with the global-scale wave model, *J. Atmos. Solar Terr. Phys.*, *64*, 1011–1035, 2002.
- Roble, R. G., On the feasibility of developing a global atmospheric model extending from the ground to the exosphere, in *Atmospheric Science Across the Stratopause*, *Geophys. Monogr. Ser.*, vol. 123, edited by D. E. Siskind, S. D. Eckermann, and M. E. Summers, pp. 53–67, AGU, Washington, D. C., 2000.
- She, C. Y., S. S. Chen, Z. L. Hu, J. Sherman, J. D. Vance, V. Vasoli, M. A. White, J. R. Yu, and D. A. Krueger, Eight-year climatology of nocturnal temperature and sodium density in the mesopause region (80 to 105 km) over Fort Collins, CO (41°N, 105°W), *Geophys. Res. Lett.*, *27*, 3289–3292, 2000.
- She, C. Y., S. S. Chen, B. P. Williams, Z. Hu, D. A. Krueger, and M. E. Hagan, Tides in the mesopause region over Fort Collins, CO (41°N, 105°W) based on lidar temperature observations covering full diurnal cycles, *J. Geophys. Res.*, *107*(18), 4350, doi:10.1029/2001JD001189, 2002.
- States, R. J., and C. S. Gardner, Influence of the diurnal tide and thermospheric heat sources on the formation of mesosphere temperature inversion layer, *Geophys. Res. Lett.*, *25*, 1483–1486, 1998.
- von Zahn, U., J. Höffner, V. Eska, and M. Alpers, The mesopause altitude: Only two distinctive levels worldwide?, *Geophys. Res. Lett.*, *23*, 3231–3234, 1996.
- Walterscheid, R., and R. Vincent, Tidal generation of the phase-locked 2-day wave in the Southern Hemisphere summer by wave-wave interaction, *J. Geophys. Res.*, *101*, 26,567–26,576, 1996.
- Yu, J. R., J. States, S. J. Franke, C. S. Gardner, and M. E. Hagan, Observations of tidal temperature and wind perturbations in the mesopause region above Urbana, IL (40°N, 88°W), *Geophys. Res. Lett.*, *24*, 1207–1210, 1997.

P. Acott, K. Arnold, D. A. Krueger, T. Li, C. Y. She, J. D. Vance, B. P. Williams, L. F. Xu, and T. Yuan, Physics Department, Colorado State University, Fort Collins, CO 80523, USA. (joeshe@lamar.colostate.edu)

T. D. Kawahara, Faculty of Engineering, Shinshu University, Nagano, Japan.

J. Sherman, Department of Physics, Indiana University of Pennsylvania, Indiana, PA 15705, USA.